



## Cytotoxicity of hepatocellular carcinoma cells to hyperthermic and ablative temperature exposures: *In vitro* studies and mathematical modelling

Goutham Reddy, Matthew R. Dreher, Christian Rossmann, Bradford J. Wood & Dieter Haemmerich

To cite this article: Goutham Reddy, Matthew R. Dreher, Christian Rossmann, Bradford J. Wood & Dieter Haemmerich (2013) Cytotoxicity of hepatocellular carcinoma cells to hyperthermic and ablative temperature exposures: *In vitro* studies and mathematical modelling, International Journal of Hyperthermia, 29:4, 318-323, DOI: [10.3109/02656736.2013.792125](https://doi.org/10.3109/02656736.2013.792125)

To link to this article: <https://doi.org/10.3109/02656736.2013.792125>



Published online: 05 Jun 2013.



Submit your article to this journal [↗](#)



Article views: 741



View related articles [↗](#)



Citing articles: 8 View citing articles [↗](#)

RESEARCH ARTICLE

# Cytotoxicity of hepatocellular carcinoma cells to hyperthermic and ablative temperature exposures: *In vitro* studies and mathematical modelling

Goutham Reddy<sup>1</sup>, Matthew R. Dreher<sup>1</sup>, Christian Rossmann<sup>2</sup>, Bradford J. Wood<sup>1</sup> and Dieter Haemmerich<sup>2,3</sup>

<sup>1</sup>Department of Radiology and Imaging Sciences, Clinical Center, Center for Interventional Oncology, National Institutes of Health, Bethesda, Maryland, <sup>2</sup>Department of Pediatrics, Medical University of South Carolina, Charleston, South Carolina, and <sup>3</sup>Department of Bioengineering, Clemson University, Clemson, South Carolina, USA

## Abstract

**Purpose:** Image-guided ablative therapies use temperatures greater than 45 °C to kill abnormal cells. There is limited published data of cell survival after ablative temperature exposures, which is of importance to predict ablation zone dimensions. The objective of this study was to determine and mathematically model survival of hepatocellular carcinoma cells following ablative temperature exposures (45–60 °C).

**Materials and methods:** Hepatocellular carcinoma (HCC) cell lines were plated in 96-well plates, and heated between 45 and 60 °C for 0–32 min. Heating was applied by a rapid media exchange with heated Hank's balanced salt solution (HBSS) in a temperature-controlled water bath. Cell viability was determined by MTS assay. Survival data was modelled by the Arrhenius model, and the thermal isoeffective dose (TID) model where kinetic parameters were determined via non-linear optimisation.

**Results:** Results suggest that the thermal dose based on cumulative equivalent minutes and parameters as used for hyperthermia exposures (<43 °C) is not applicable for ablative exposures. We found  $R = 0.72$  for temperatures between 45–60 °C for the TID model. The Arrhenius parameters were frequency factor  $A = 3.25E43$  1/s, and activation energy  $E_a = 281$  kJ/mol. These parameters correlate well with a prior study in the same cell line, and with threshold temperatures for necrosis from *in vivo* studies.

**Conclusions:** Our results suggest that standard TID model kinetic parameters based on hyperthermia studies, often also used at ablation temperatures, are not applicable at these higher temperatures for HCC cells.

## Keywords

Ablation, hyperthermia, modelling, thermal dose

## History

Received 20 December 2012

Revised 10 March 2013

Accepted 30 March 2013

Published online 5 June 2013

## Introduction

Image-guided ablative therapies are increasingly being used in clinical treatment of tumours in the liver, kidney, prostate, lung, and other sites [1–3]. Distinct from traditional hyperthermia treatments (37–45 °C for up to 1 h), thermal ablation operates at up to 150 °C with shorter exposure times between ~1 and 30 min. Energy sources available for achieving tumour destruction by focal ablation include radiofrequency (RF), laser, microwave, and high intensity focused ultrasound (HIFU) [4,5]. In particular, radiofrequency ablation (RFA) is a valuable technique to obtain local control of unresectable tumours of the liver, kidney, prostate, and other organs. Note that ablative technologies generally produce a spatial gradient of temperatures in the target region. For this reason it is important to understand and quantify thermally induced

damage in biological cells and tissue for the design of optimal thermal therapy protocols.

Various assays have been used to quantify cell injury after hyperthermic injury *in vitro*, including clonogenic and dye exclusion assays, functional assays based on enzyme activity, and dye uptake [6–12]. The type of assay used greatly impacts results [6,7,11], and a recent study suggests that dye uptake-based assays are predictive of *in vivo* survival quantified by histology [11]. Furthermore, there exists limited *in vitro* data from different assays at temperatures above 45 °C with short duration of heating [8,9,11–15].

The Arrhenius model is a mathematical description based on first order kinetics to predict cell survival after subjecting cells to a particular temperature history [16], and is commonly used for predicting thermal damage after ablation exposures [6–9,11,15,17,18]. The thermal isoeffective dose (TID) model is a formulation derived from the Arrhenius model, and commonly used in the hyperthermia field [16]. Numerous prior studies confirm the ability to accurately predict cell death resulting from hyperthermia exposures by an Arrhenius relationship with two distinct regions of

Correspondence: Dieter Haemmerich, Department of Pediatric Cardiology, Medical University of South Carolina, 165 Ashley Avenue, PO Box 250915, Charleston, SC 29425, USA. Tel: +1 843 792 1396. E-mail: haemmerich@ieee.org

sensitivity (i.e. different activation energies) above and below 43 °C. However, Arrhenius models based on experimental data acquired at hyperthermic exposures may not accurately predict cell death resulting from high temperature (i.e. thermal ablation) exposures. Specifically, the Arrhenius model parameters (activation energy and frequency factor) calculated from long duration, low-temperature hyperthermia exposures (<45 °C) likely do not accurately predict cell death resulting from shorter duration, high temperature exposures [11].

The second commonly employed thermal damage model is the TID model, where an equivalent heating duration at a reference temperature (typically 43 °C) is calculated. In the TID model, a cumulative equivalent heating time (e.g. cumulative equivalent minutes at 43 degrees Celsius, CEM43 °C (min)) is determined based on the temperature history. The parameters for the TID model are derived from extended exposures at hyperthermic temperatures, and similar to prior Arrhenius models, may not be applicable to ablation temperature exposures.

The objective of this study was to measure survival of hepatocellular carcinoma cells following short duration, (30 s to 32 min) high temperature exposures (45–60 °C) using a tetrazolium-based survival assay. These survival data may be used to better predict cell survival after ablative temperature exposures.

## Methods

*In vitro* experiments were performed on hepatocellular carcinoma (HCC) cells and cell viability was measured after the high temperature exposures at specified intervals within the next 24 h. Subsequently, the viability data was used to calculate the cell survival fraction as a function of temperature and exposure time for each experiment. Based on the experimental survival fraction data and measured temperature, an Arrhenius model was fitted to predict cell death for high temperature exposures.

## *In vitro* experiments

Cytotoxicity: HepG2 HCC cell lines were plated in 96-well plates (~2000 cells/well). Cells were heated between 45° and 60 °C for 30 s, 1, 2, 4, 8, 16, or 32 min. The thermal exposures were applied by a rapid media exchange with heated Hank's balanced salt solution (HBSS) in a temperature-controlled water bath (see Figure 1). Cell viability was determined by tetrazolium-based (MTS) assay (Promega, Madison, WI) at 5 min, 30 min, 1, 2, 4, and 24 h. For mathematical modelling, that data at 2 h was used as there was no significant change in survival following 2 h (data not shown). Experiments were carried out in triplicate at each temperature and time point. Total number of cells was counted based upon morphology using a haemocytometer grid.

## Mathematical model

### *Arrhenius model*

The Arrhenius formulation characterizes thermal tissue damage with a first order irreversible kinetic relationship, which relates temperature and exposure time and is given with:

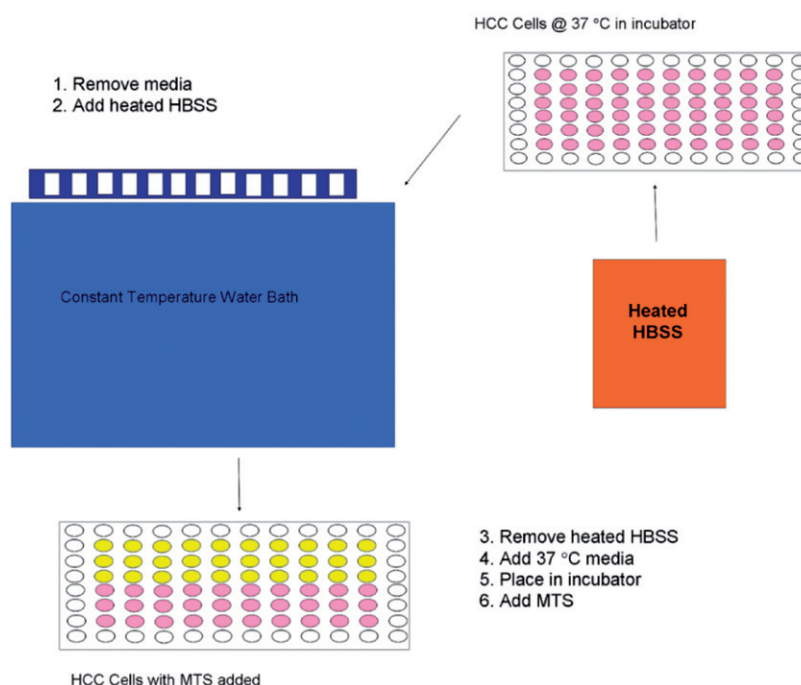
$$S = e^{-\int_0^t k dt} \quad (1)$$

$$k = Ae^{\left(-\frac{E_a}{RT}\right)} \quad (2)$$

where  $S$  (%) is the cell survival fraction,  $T$  (K) is the heating temperature,  $t$  (s) is the time  $k$  is the injury rate ( $s^{-1}$ ),  $E_a$  ( $kJ\ mol^{-1}$ ) is the activation energy,  $A$  ( $s^{-1}$ ) is the frequency factor and  $R$  ( $8.314\ J\ mol^{-1}\ K^{-1}$ ) is the universal gas constant.

To fit the model to the experimental data, we used MATLAB to estimate the kinetic parameters  $A$ , and  $E_a$  via a non-linear optimisation method (Nelder-Mead

Figure 1. Schematic sketch of the experimental set-up. HCC cell lines were plated in well plates and exposed to temperatures between 45–60 °C for 0.5 to 32 min. After heating, cell viability was determined by tetrazolium-based (MTS) assay.



Simplex method [19]). A least-square error function was defined that calculates the difference between the experimental data and the fitted data provided by the Arrhenius model. The objective function to be minimized was given as:

$$f(X) = \left[ \frac{1}{N} \sum_{i=1, N} (S_{\text{exp},i}(X) - S_{\text{func},i}(X))^2 \right]^{0.5} \quad (3)$$

where  $N$  is the total number of experimental points,  $X$  is a vector containing all independent optimisation variables,  $S_{\text{exp},i}$  represents the experimentally measured survival fraction data and  $S_{\text{func},i}$  represents the calculated data at each measured point in time. While most other studies assumed constant temperature to model isothermal hyperthermic injury, here we corrected for variation of temperature during cell exposure similar to two recent studies [9,14]. Due to media addition, temperature varies around the target temperature ( $\pm 1.4^\circ\text{C}$ ) and might influence survival fraction. We considered the thermal history recorded from the experiments during the parameter fitting.

#### Thermal isoeffective dose (TID) model

The TID model is based on the Arrhenius formulation, but assumes that temperature varies only within a small range (e.g. as applies to hyperthermia exposures) [16]. The goal of the TID model is to derive an equivalent exposure time (thermal dose) at a reference temperature (typically  $43^\circ\text{C}$ ) from the actual temperature history. The TID is a widely used model for assessing hyperthermia treatments and is measured in cumulative equivalent minutes at  $43^\circ\text{C}$  ( $\text{CEM}_{43}$ ). Depending on the thermal temperature history the thermal dose is calculated via:

$$\text{CEM}_{43} = \sum_{i=1}^N [R_{\text{CEM}}]^{(43-T_i)} t_i \quad (4)$$

where  $R_{\text{CEM}}$  is a dimensionless compensation factor,  $T_i$  ( $^\circ\text{C}$ ) is the constant temperature which is applied for the time  $t_i$  (min). The majority of prior studies use different values for  $R_{\text{CEM}}$  for two different temperature ranges; 0.25 for temperatures below, and 0.5 for temperatures greater  $43^\circ\text{C}$  [20]. As presented by Sapareto and Dewey [16],  $R_{\text{CEM}}$  can be calculated as a function of the activation energy and absolute temperature from an Arrhenius model with:

$$R_{\text{CEM}} = e^{\frac{E_a}{R(T+1)}} \quad (5)$$

where  $E_a$  (sometimes referred as  $\Delta H$ ) ( $\text{kJ mol}^{-1}$ ) is the activation energy,  $R$  is the universal gas constant ( $8.314 \text{ J K}^{-1} \text{ mol}^{-1}$ ) and  $T$  ( $^\circ\text{K}$ ) is the absolute temperature.

In the current study we calculated the compensation factor  $R_{\text{CEM}}$  of the TID model for ablative temperature ranges for comparison with values of prior studies. Since the TID implicitly assumes temperature during exposure stays within a narrow range (note that  $T$  is a constant in Equation 5), we calculated  $R_{\text{CEM}}$  for two temperature ranges ( $45\text{--}50^\circ\text{C}$ , and  $50\text{--}60^\circ\text{C}$ ).

## Results

### In vitro experiments

With hyperthermia exposures it is challenging to immediately elevate and control temperature using rapid media exchange. Initially, there is decrease in temperature following media addition, then a temperature increase due to heating from the hot water bath in which the tissue culture plate was suspended. Figure 2 depicts the thermal history used to calculate the Arrhenius relationship for each temperature condition.

In Figure 3 the survival fraction as a function of temperature and exposure time is depicted. Increasing temperature and exposure time decreased cell survival for all temperatures greater  $45^\circ\text{C}$ . Based on the experimental data, we found that cell death was minimal at all  $45^\circ\text{C}$  exposure times. With increasing exposure time up to 8 min, a monotonic decrease in survival was measured for temperatures between  $50\text{--}52.5^\circ\text{C}$ . For the same temperature range, near or complete cell death (survival fraction  $<24\%$ ) was found at exposure times  $>8$  min. No clear trend in survival could be observed at  $45^\circ\text{C}$  target temperature. Most likely these fluctuations are the result from the high variability in the data at  $45^\circ\text{C}$  (note large error bars). Additional factors include the relatively larger temperature variations in the experiments at  $45^\circ\text{C}$  target temperature (Figure 2), as well as possible thermotolerance effects.

### Mathematical model

An Arrhenius model was used to characterise the thermal injury; the two kinetic parameters – activation energy ( $E_a$ ) and frequency factor ( $A$ ) – were determined via model fit to the experimental data. Figure 4 shows the prediction of the Arrhenius model between  $45\text{--}60^\circ\text{C}$  in comparison to data points from the *in vitro* study.

Table 1 lists the fitted Arrhenius parameters. Based on these parameters, Equation (5) was used to calculate the compensation factor  $R$  for further comparison with values of prior studies. The  $R$  values 0.716 and 0.72 calculated for the temperature ranges  $45\text{--}50^\circ\text{C}$  and  $50\text{--}60^\circ\text{C}$  were noticeably greater than previously proposed values of 0.25 and 0.5.

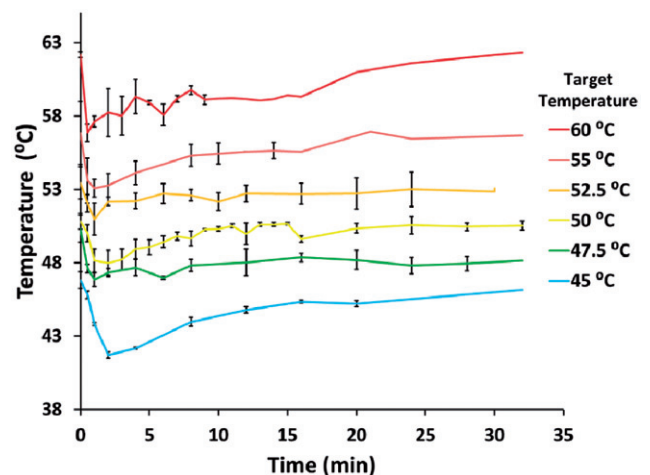


Figure 2. Temperature variations of the experiments recorded over 32 min. An initial decrease (time  $<3$  min) was noted due to the media addition in the assay. Error bars indicate the standard deviation.



Figure 3. Survival fraction as a function of temperature and exposure time. The error bars indicate  $\pm$  standard error of mean.

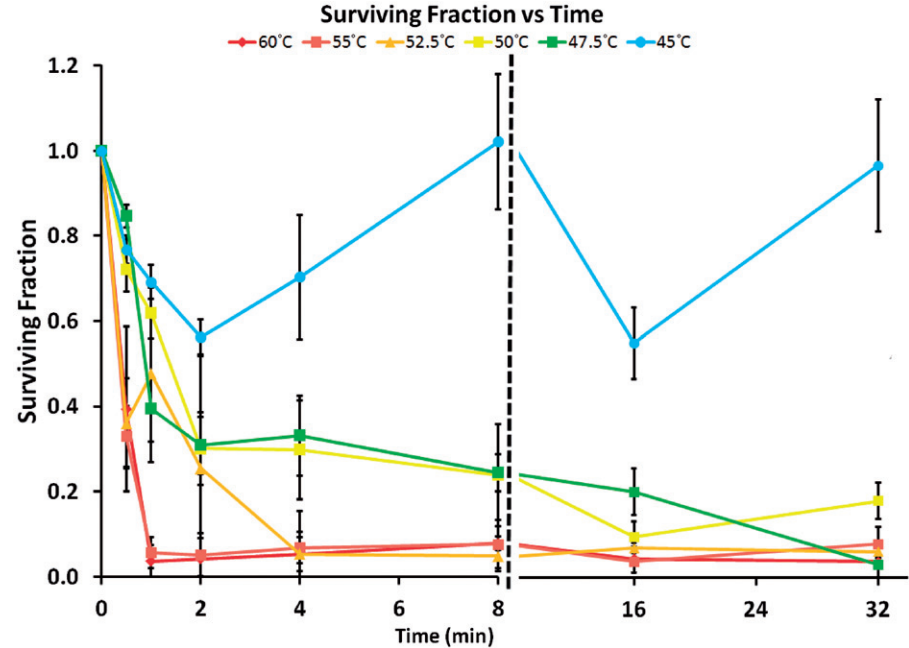


Figure 4. Points show the measured surviving fraction based on a tetrazolium survival assay. Solid line: prediction of surviving fraction via Arrhenius model for heating 0–10 min. Note: The sigmoidal shape of the 45 °C curve is due to considerable temperature variation within the first 10 min (see Figure 2).

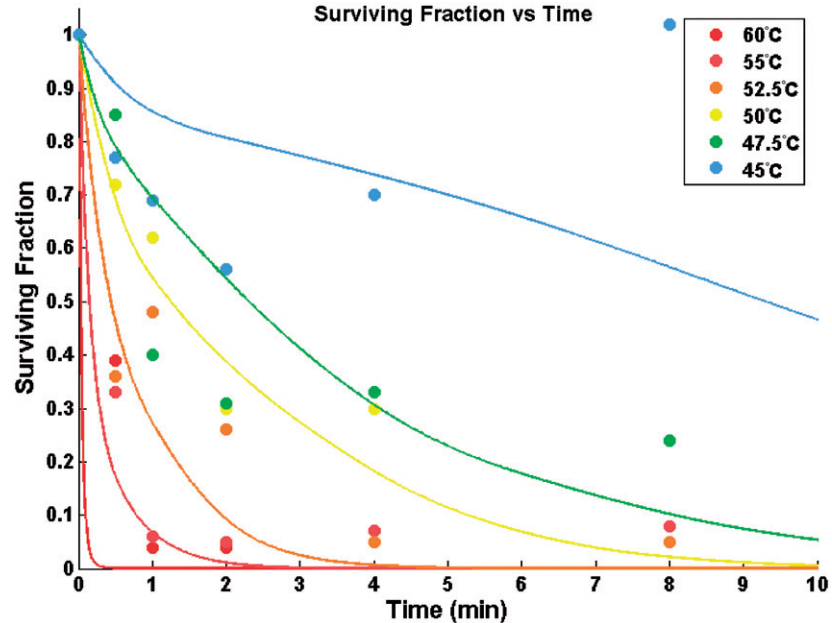


Table 1. Fitted Arrhenius parameters as well as compensation factor (R) derived from the fitted model parameters compared with prior R values.

Temperature (°C)	Frequency factor A (1/s)	Activation energy E <sub>a</sub> (kJ/mol)	R current study	R Sapareto [16]
37–43	–	–	–	0.25
43–45	–	–	–	0.50
45–50	3.247·10 <sup>43</sup>	281.4	0.716	0.50
50–60			0.724	0.50

Discussion

Super-physiological temperatures are used in traditional hyperthermia treatment in brain, bone and recurrent breast tumours and superficial lesions such as melanoma and neck nodes [21–24]. Although traditional mild hyperthermia

treatment by itself is generally ineffective, it noticeably improves effects of chemo- and radiotherapy [25–28]. Traditional mild hyperthermia uses elevated temperature in the range of 40–45 °C which is typically applied for up to 1 h. While in the past, due to difficulties of heating deep-seated tumours, hyperthermia treatment has been limited to superficial lesions [29], improvements of heating devices and optimisation of heating methodology facilitated better heating of deep-seated tumours [30]. Thermal ablation is, similarly to hyperthermia, based on tissue heating, but employs considerably higher temperatures (~50–100 °C) for typically a few minutes. The high temperatures cause rapid cell death and introduce coagulative necrosis of the target tissue while surrounding healthy tissue remains mostly unaffected. Treatment modalities such as radio-frequency, microwave and high intensity focused ultrasound

ablation allow thermal energy delivery to deep-seated tumours in liver, lung, bone, prostate, kidney and breast [31–34]. Particularly thermal ablation therapies are often used for patients that are not eligible for surgical resection for tumours where chemo- and radiation therapy are not effective, such as those in the liver.

In order to design and optimise thermal therapy protocols it is of relevance to understand and quantify thermally induced damage in biological cells and tissue. Prior studies investigated the kinetics of thermal injury of prostate cancer and renal carcinoma cells at temperatures from 37–50 °C using clonogenic assays [7,9,14]. While the clonogenic assay is the preferred technique for standard cell survival analysis, it is difficult to obtain the experimental results at temperatures higher than 50 °C. There is limited injury data at high temperatures [9,12,15], in part because accurate extraction of kinetic parameters requires ideally isothermal exposures which are difficult to maintain with water bath-based viability assays. In the current study we modified the assay to reduce the non-isothermal portion and provide results at ablative temperatures.

Prior reported kinetic parameters vary by species, cell type, and assay used to assess injury. Values for the activation energy  $E_a$  have been reported between 350–550 kJ/mol and  $R$  values between 0.55 and 0.70 for prostate cancer cells, 203 kJ/mol and 0.82 for benign hyperplastic prostate tissue, and >550 kJ/mol and  $R > 0.7$  for renal cell carcinoma using dye exclusion assays [11], and one study in the same HCC cell line (HepG2) studied here reported activation energy of 257–272 kJ/mol, depending on heating rate [15].  $E_a$  calculated in this study (see Table 1) (281.4 kJ/mol) is within the range of these prior reported values but noticeably lower than values for prostate cancer and renal cell carcinoma cells.

The data resulting from such studies highly depend on the particular assay used [11]. For example for the HCC cell line studied here, one prior study using a dye-based assay showed results similar to ours [15], while another study using an assay based on enzyme activity suggests much higher survival [12]. Importantly, He et al. [11] note in a prior study that model comparison should only be done between studies with the same classes of assays, and found that dye uptake assays such as used here provide similar kinetic parameters as the gold standard method histology for the two cell and tissue types where they had data for such comparison (AT-1 cells and benign prostatic hyperplasia tissue). Results from clonogenic assays often produce very high activation energy (~350–1600 kJ/mol) whereas it is generally lower for histology and dye viability assays (~100–800 kJ/mol) [35,36]. This suggests that dye-based assays may be a valid choice in prediction of *in vivo* response, which is ultimately the most important measure.

Some studies demonstrate an initial region where cell viability does not change much (shoulder region), and where the Arrhenius and TID models thus do not provide a good fit [12,37]. Notably, depending on assay type, this shoulder region may or may not be present, even in the same cell type [6,7], again highlighting the importance of appropriate assay choice. While we did not observe any clear shoulder regions in our data, other investigators developed models to represent data where such a shoulder is present [10,12].

It is known from the hyperthermia literature that different activation energies correspond to different temperature ranges [16]. Specifically, the Arrhenius parameters (activation energy and frequency factor) calculated from long duration, low temperature hyperthermia exposures (<45 °C) likely do not accurately predict cell death resulting from shorter duration, high temperature exposures [11]. In agreement with this notion, the calculated values for  $R$  in this study ( $R \sim 0.72$ , see Table 1) for temperatures between 45–60 °C are considerably higher than values derived from hyperthermia studies ( $R = 0.5$  for  $T > 43$  °C). Importantly, the mathematical model derived from this study predicts near complete cell death (<10% survival) after exposure to 52.5 °C for 5 min. This is in agreement with prior *in vivo* studies in a rat tumour model where a threshold temperature of 52 °C for necrosis was reported for 5 min ablation [38]. This further suggests that the use of the TID model with  $R = 0.5$  is not appropriate to predict damage at ablative temperatures.

Ablative devices create a temperature gradient with temperatures ~50–55 °C presenting in proximity of the ablative margin [8,38]. While there are no *in vivo* data available for direct comparison in the same HCC cell line used in the current study, our results are in general agreement with time and temperatures at the ablation zone boundary of these prior studies. For example in kidney, *in vivo* peak temperatures of 54° and 57 °C (with >6–8 min above 50 °C) were measured at the boundary of chronic and acute necrosis zones, respectively [8]. In our study it took ~2 min to kill 90% of cells at 52.5 °C, and ~1 min at 55 °C, which is a similar range to prior *in vivo* findings.

## Conclusions

Our *in vitro* studies show cell survival after exposures to ablative temperatures between 45–60 °C, and derived kinetic model parameters that agree well with a prior study that used a similar assay in the same cell line [15]. Our results suggest that standard TID model kinetic parameters based on hyperthermia studies [16] and often also used at ablation temperatures are not applicable at these higher temperatures.

## Declaration of interest

This work was supported by US National Institutes of Health (NIH) grant R01CA118990 to D.H., and by the NIH Center for Interventional Oncology and NIH Intramural Research Program. The work was conducted in a facility constructed with support from the NIH, grant C06 RR018823 from the Extramural Research Facilities Program of the National Center for Research Resources. The authors alone are responsible for the content and writing of the paper.

## References

1. Lees WR, Gillams A. Radiofrequency ablation: Other abdominal organs. *Abdom Imaging* 2005;30:451–5.
2. Gillams AR. Should hepatocellular carcinoma be ablated or resected? *Nat Clin Pract Gastroenterol Hepatol* 2007;4:586–7.
3. Gillams A. Tumour ablation: Current role in the kidney, lung and bone. *Cancer Imaging* 2009;9A:S68–70. doi: 10.1102/1470-7330.2009.9028.

4. Stone MJ, Wood BJ. Emerging local ablation techniques. *Semin Intervent Radiol* 2006;23:85–98.
5. Dorfman GS, Lawrence TS, Matrisian LM. The translational research working group developmental pathway for interventional devices. *Clin Cancer Res* 2008;14:5700–6.
6. Bhowmick S, Swanlund DJ, Bischof JC. Supraphysiological thermal injury in Dunning AT-1 prostate tumor cells. *J Biomech Eng* 2000;122:51–9.
7. Bhowmick S, Coad JE, Swanlund DJ, Bischof JC. In vitro thermal therapy of AT-1 Dunning prostate tumours. *Int J Hyperthermia* 2004;20:73–92.
8. He X, McGee S, Coad JE, Schmidlin F, Iaizzo PA, Swanlund DJ, et al. Investigation of the thermal and tissue injury behaviour in microwave thermal therapy using a porcine kidney model. *Int J Hyperthermia* 2004;20:567–93.
9. He X, Bischof JC. The kinetics of thermal injury in human renal carcinoma cells. *Ann Biomed Eng* 2005;33:502–10.
10. Feng Y, Tinsley Oden J, Rylander MN. A two-state cell damage model under hyperthermic conditions: Theory and in vitro experiments. *J Biomech Eng* 2008;130:041016. doi: 10.1115/1.2947320.
11. He X, Bhowmick S, Bischof JC. Thermal therapy in urologic systems: A comparison of Arrhenius and thermal isoeffective dose models in predicting hyperthermic injury. *J Biomech Eng* 2009;131:074507. doi: 10.1115/1.3128671.
12. O'Neill DP, Peng T, Stiegler P, Mayrhauser U, Koestenbauer S, Tscheliessnigg K, et al. A three-state mathematical model of hyperthermic cell death. *Ann Biomed Eng* 2011;39:570–9.
13. Hilger I, Rapp A, Greulich KO, Kaiser WA. Assessment of DNA damage in target tumor cells after thermoablation in mice. *Radiology* 2005;237:500–6.
14. He X, Wolkers WF, Crowe JH, Swanlund DJ, Bischof JC. In situ thermal denaturation of proteins in Dunning AT-1 prostate cancer cells: Implication for hyperthermic cell injury. *Ann Biomed Eng* 2004; 32:1384–98.
15. Shah B, Bhowmick S. Evaluation of important treatment parameters in supraphysiological thermal therapy of human liver cancer HepG2 cells. *Ann Biomed Eng* 2006; 34:1745–57.
16. Sapareto SA, Dewey WC. Thermal dose determination in cancer therapy. *Int J Radiat Oncol Biol Phys* 1984; 10:787–800.
17. Pearce J, Liao WH, Thomsen S. The kinetics of thermal damage: Estimation and evaluation of model coefficients. In: *ASME Conference Proceedings, Advances in Heat and Mass Transfer Biotechnology*. Fairfield, NJ, ASME, 1998, HTD-362/BED-40, pp. 71–75.
18. Diller KR, Pearce JA. Issues in modeling thermal alterations in tissues. *Ann NY Acad Sci* 1999;888:153–64.
19. Lagarias JC, Reeds JA, Wright MH, Wright PE. Convergence properties of the nelder-mead simplex method in low dimensions. *SIAM J Optim* 1998;9:112–47.
20. Prakash P, Diederich CJ. Considerations for theoretical modelling of thermal ablation with catheter-based ultrasonic sources: Implications for treatment planning, monitoring and control. *Int J Hyperthermia* 2012;28:69–86.
21. Salcman M, Samaras GM. Hyperthermia for brain tumors: Biophysical rationale. *Neurosurgery* 1981;9:327–35.
22. Ikenaga M, Ohura K, Yamamuro T, Kotoura Y, Oka M, Kokubo T. Localized hyperthermic treatment of experimental bone tumors with ferromagnetic ceramics. *J Orthop Res* 1993;11:849–55.
23. Vernon CC, Hand JW, Field SB, Machin D, Whaley JB, van der Zee J, et al. Radiotherapy with or without hyperthermia in the treatment of superficial localized breast cancer: Results from five randomized controlled trials. International collaborative hyperthermia group. *Int J Radiat Oncol Biol Phys* 1996;35:731–44.
24. Falk MH, Issels RD. Hyperthermia in oncology. *Int J Hyperthermia* 2001;17:1–18.
25. Hahn GM. Potential for therapy of drugs and hyperthermia. *Cancer Res* 1979;39:2264–8.
26. Seegenschmiedt HM, Karlsson UL, Sauer R, Brady Jr LW, Herbst M, Amendola BE, et al. Superficial chest wall recurrences of breast cancer: Prognostic treatment factors for combined radiation therapy and hyperthermia. *Radiology* 1989;173:551–8.
27. Hiraoka M, Masunaga S, Nishimura Y, Nagata Y, Jo S, Akuta K, et al. Regional hyperthermia combined with radiotherapy in the treatment of lung cancers. *Int J Radiat Oncol Biol Phys* 1992;22: 1009–14.
28. Partanen A, Yarmolenko PS, Viitala A, Appanaboyina S, Haemmerich D, Ranjan A, et al. Mild hyperthermia with magnetic resonance-guided high-intensity focused ultrasound for applications in drug delivery. *Int J Hyperthermia* 2012;28:320–36.
29. Nielsen OS, Horsman M, Overgaard J. A future for hyperthermia in cancer treatment? *Eur J Cancer* 2001;37:1587–9.
30. Hiraoka M, Abe M. Current status of hyperthermia for deep-seated tumors [in Japanese]. *Gan To Kagaku Ryoho* 1989;16:289–96.
31. Abdalla EK, Vauthey JN, Ellis LM, Ellis V, Pollock R, Broglio KR, et al. Recurrence and outcomes following hepatic resection, radiofrequency ablation, and combined resection/ablation for colorectal liver metastases. *Ann Surg* 2004;239:818–25.
32. Illing RO, Kennedy JE, Wu F, ter Haar GR, Protheroe AS, Friend PJ, et al. The safety and feasibility of extracorporeal high-intensity focused ultrasound (HIFU) for the treatment of liver and kidney tumours in a Western population. *Br J Cancer* 2005;93: 890–5.
33. Simon CJ, Dupuy DE, Mayo-Smith WW. Microwave ablation: Principles and applications. *Radiographics* 2005;25:S69–83.
34. Kojima H, Tanigawa N, Kariya S, Komemushi A, Shomura Y, Sawada S. Clinical assessment of percutaneous radiofrequency ablation for painful metastatic bone tumors. *Cardiovasc Intervent Radiol* 2006;29:1022–6.
35. Schutt DJ, Swindle MM, Helke KL, Bastarrika G, Schwarz F, Haemmerich D. Sequential activation of ground pads reduces skin heating during radiofrequency tumor ablation: In vivo porcine results. *IEEE Trans Biomed Eng* 2010;57:746–53.
36. He X. Thermostability of biological systems: Fundamentals, challenges, and quantification. *Open Biomed Eng J* 2011;5:47–73.
37. Sapareto SA, Hopwood LE, Dewey WC, Raju MR, Gray JW. Effects of hyperthermia on survival and progression of chinese hamster ovary cells. *Cancer Res* 1978;38:393–400.
38. Solazzo S, Mertyna P, Peddi H, Ahmed M, Horkan C, Goldberg SN. RF ablation with adjuvant therapy: Comparison of external beam radiation and liposomal doxorubicin on ablation efficacy in an animal tumor model. *Int J Hyperthermia* 2008;24:560–7.
39. Hahn GM, Li GC. Thermotolerance and heat shock proteins in mammalian cells. *Radiat Res* 1982;92:452–7.
40. Li GC, Fisher GA, Hahn GM. Induction of thermotolerance and evidence for a well-defined, thermotropic cooperative process. *Radiat Res* 1982;89:361–8.
41. Altrogge I, Preusser T, Kroger T, Buskens C, Pereira PL, Schmidt D, et al. Multiscale optimization of the probe placement for radiofrequency ablation. *Acad Radiol* 2007;14:1310–24.
42. Payne S, Flanagan R, Pollari M, Alhonnoro T, Bost C, O'Neill D, et al. Image-based multi-scale modelling and validation of radio-frequency ablation in liver tumours. *Philos Transact A Math Phys Eng Sci* 2011;369:4233–54.
43. Rossmann C, Rattay F, Haemmerich D. Platform for patient-specific finite-element modeling and application for radiofrequency ablation. *Visualization, Image Processing and Computation in Biomedicine* 2012;1. DOI: 10.1615/2012004898.
44. Goldberg SN, Gazelle GS. Radiofrequency tissue ablation: Physical principles and techniques for increasing coagulation necrosis. *Hepatoenterology* 2001;48:359–67.
45. Mertyna P, Hines-Peralta A, Liu ZJ, Halpern E, Goldberg W, Goldberg SN. Radiofrequency ablation: Variability in heat sensitivity in tumors and tissues. *J Vasc Interv Radiol* 2007;18:647–54.
46. Mertyna P, Dewhurst MW, Halpern E, Goldberg W, Goldberg SN. Radiofrequency ablation: The effect of distance and baseline temperature on thermal dose required for coagulation. *Int J Hyperthermia* 2008;24:550–9.